

Supporting Information

A porous hybrid material based on calixarene dye and TiO₂ demonstrating high and stable photocatalytic performance

Yi-Fan Chen,^{a,b} Jian-Feng Huang,^a Min-Hui Shen,^a Jun-Min Liu,^{a, *} Li-Bo Huang,^a
Yu-Hui Zhong,^a Su Qin,^a Jing Guo,^a Cheng-Yong Su^{a, *}

^a School of Chemistry and School of Materials Science and Engineering, Sun Yat-sen
University, Guangzhou, 510275, China.

^b Hainan Provincial Key Lab of Fine Chem, School of Chemical Engineering and
Technology, Hainan University, Haikou, 570228, China.

Corresponding authors:

liujunm@mail.sysu.edu.cn (J.-M. Liu); cesscy@mail.sysu.edu.cn (C.-Y. Su).

Contents

1. Fig. S1. Synthesis of HO-TPA	S4
2. Fig. S2. Synthesis of HO-TPA-TiO ₂	S8
3. Fig. S3. PXRD patterns recorded in the formation process of HO-TPA-TiO ₂	S8
4. Fig. S4. N ₂ sorption isotherms of HO-TPA-TiO ₂ system at 77K.....	S9
5. Fig. S5. N ₂ sorption isotherms of Pt/HO-TPA-TiO ₂ , HO-TPA-TiO ₂ with 500 °C calcination, Gel-TiO ₂ and P25-TiO ₂ at 77 K.....	S10
6. Fig. S6. The pore size distribution of HO-TPA-TiO ₂ system.....	S11
7. Fig. S7. SEM images of HO-TPA-TiO ₂	S11
8. Fig. S8. XPS measurement for Gel-TiO ₂	S12
9. Fig. S9. XPS measurement for HO-TPA-TiO ₂	S13
10. Fig. S10. EDX spectrum of Pt/HO-TPA-TiO ₂	S13
11. Fig. S11. XPS measurement for ReP.....	S14
12. Fig. S12. XPS measurement for ReP/HO-TPA-TiO ₂ after photocatalysis.....	S15
13. Fig. S13. The bonding mode between HO-TPA and TiO ₂	S16
14. Fig. S14. Mott-Schottky plot of Gel-TiO ₂	S16
15. Fig. S15. Cyclic voltammogram of HO-TPA	S17
16. Fig. S16. UV-vis absorption spectra and photoluminescence spectra of HO-TPA in CH ₂ Cl ₂ (E ₀₋₀ = 1240/λ _{int}). ...	S17
17. Fig. S17. Cyclic voltammogram of ReP in 0.1 M TBAPF ₆ of THF solutions measured with a scan rate of 100 mV s ⁻¹	S18
18. Fig. S18. UV-vis diffraction and steady-state solid photoluminescence spectra of HO-TPA-TiO ₂ (2.5/5.0/7.5 wt%).....	S18
19. Fig. S19. The color of the dye doping shedding from Pt/Gel-TiO ₂ /HO-TPA (2.4 wt%) and HO-TPA-TiO ₂ (5 wt%).....	S20
20. Fig. S20. Photocatalytic action spectrum for H ₂ evolution after 1 h irradiation under 400, 420, 450, 470, and 515 nm LED light source.....	S21

21. Fig. S21. Steady-state solid photoluminescence spectra of the HO-TPA, physical-mixing Gel-TiO ₂ /HO-TPA, dye-sensitized Gel-TiO ₂ /HO-TPA, and hybrid HO-TPA-TiO ₂	S21
22. Fig. S22. ¹³ C NMR spectra of ¹³ CO ₂ and ¹³ CO before and after irradiation.....	S22
23. Fig. S23. GC-MS spectra of ReP/HO-TPA-TiO ₂ dispersion in ¹² CO ₂ , and ¹³ CO ₂ -saturated DMF.....	S23
24. Fig. S24. Possible chemical processes for the two-electron reduction of CO ₂ to CO catalyzed by a Re(I) complex (PReX).....	S23
25. Table S1. BET surface area, pore volume and pore width of HO-TPA-TiO ₂ system derived from 77 K N ₂ sorption isotherms.....	S24
26. Table S2. Electrochemical properties of compounds used in this study (V vs. Ag/AgCl).....	S24
27. Table S3. AQY results of Pt/HO-TPA-TiO ₂ (5.0 wt%) after 1h irradiation under 450 nm LED light source.....	S25
28. Table S4. AQY results of some reported heterogeneous catalytic systems in photocatalytic H ₂ production studies.....	S25
29. Table S5. The apparent quantum yields on photocatalytic CO production for ReP/HO-TPA-TiO ₂ (5.0 wt%) at 420, 450 nm and 500 nm.....	S26

Experimental details

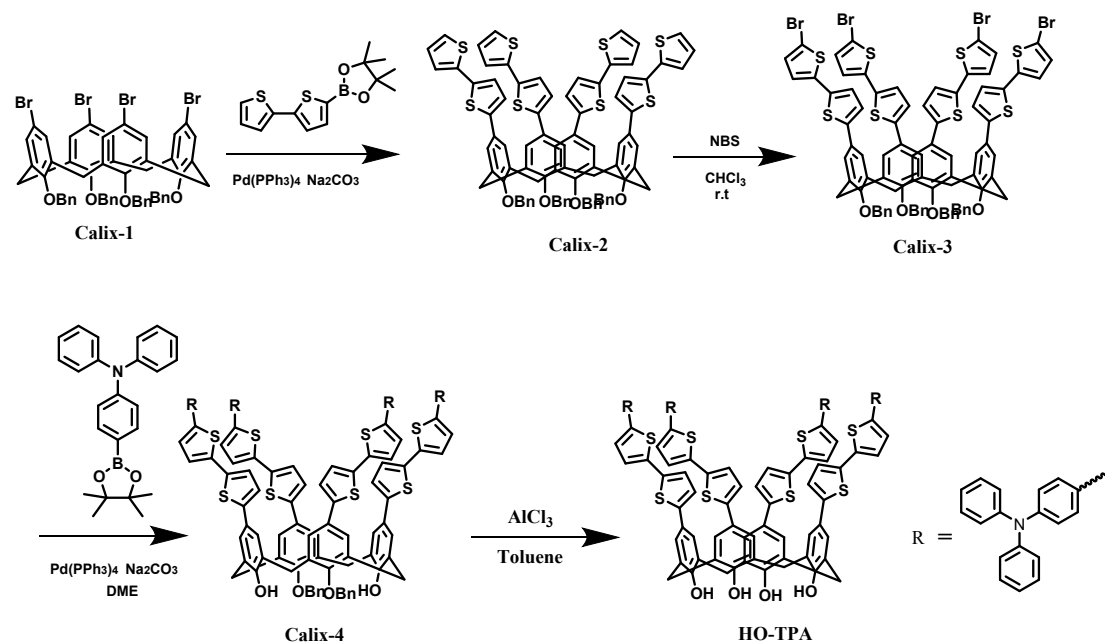


Fig. S1. The synthesis of **HO-TPA**.

Synthesis of Calix-2

Calix-1 (800 mg, 0.727 mmol), 5-(4,4,5,5-Tetramethyl-1,3,2-dioxaborolan-2-yl)-2,2'-bithiophene (1.06 g, 3.635 mmol), $\text{Pd}(\text{PPh}_3)_4$ (250 mg, 0.2181 mmol), and K_2CO_3 (5.53 g, 40.0 mmol) aqueous solution were added to a flask under nitrogen atmosphere, and then dimethoxyethane (100 mL) was added. The reaction mixture was refluxed at 90 °C for overnight, and then cooled and evaporated to dryness. The residue was dissolved in dichloromethane and the organic content was washed with water and saturated brines, and subsequently dried over anhydrous MgSO_4 , filtered and evaporated to afford a crude product which was further purified by silica-gel column chromatography using petroleum ether and ethyl acetate as the eluent (10:1, v/v) to yield 911 mg light yellow solid. Yield: 87%. ^1H NMR (400 MHz, CDCl_3 , δ): 7.31 (s, 4H), 7.29 (s, 8H), 7.24-7.23(m, 8H), 7.09 (d, $J = 4.8$ Hz, 8H), 7.02 (d, $J = 3.2$ Hz, 4H), 6.90 (t, $J = 4.4$ Hz, 4H), 6.86 (s, 8 H), 6.79 (d, $J = 3.6$ Hz, 8H), 6.70 (d, $J = 4.0$ Hz, 4H), 4.97 (s, 8H), 4.17 (d, $J = 13.2$ Hz, 4H), 2.94 (d, $J = 13.6$ Hz, 4H); ^{13}C -

NMR (100 MHz, CDCl₃, δ): 155.29, 143.28, 137.42, 135.60, 135.41, 129.95, 128.59, 128.29, 128.21, 127.77, 125.67, 124.57, 123.81, 123.18, 122.64, 76.80, 31.53; MALDI-TOF: m/z 1441.2527 ([M + H]⁺); 1463.2357 ([M + Na]⁺).

Synthesis of Calix-3

Calix-2 (247 mg, 0.172 mmol) and 1-bromo-2,5-pyrrolidinedione (125 mg, 0.703 mmol) were stirred in chloroform at room temperature for 10 h. The mixture was cooled and evaporated to dryness. The residue was extracted with dichloromethane and the combined organic extracts were washed with water and brine, and then dried over anhydrous MgSO₄, filtered and evaporated to afford a crude product which was further purified by silica-gel column chromatography with a mixture of petroleum ether and dichloromethane as the eluents (5:1, v/v) to yield 277 mg yellow solid. Yield: 92%. ¹H NMR (400 MHz, CDCl₃, δ) 7.32-7.30 (m, 8H), 7.29 (s, 4H), 7.27 (s, 4H), 7.26 (s, 4H), 6.87 (d, J = 4.0 Hz, 4H), 6.84 (s, 8H), 6.77 (d, J = 3.6 Hz, 4H), 6.72 (m, 8H), 4.98 (s, 8H), 4.18 (d, J = 13.2 Hz, 4H), 2.94 (d, J = 13.6 Hz, 4H); ¹³C-NMR (100 MHz, CDCl₃, δ): 155.46, 143.81, 139.33, 137.33, 135.69, 134.54, 130.61, 130.04, 129.95, 129.86, 128.37, 128.32, 128.28, 125.70, 124.65, 123.12, 122.64, 110.45, 76.82, 31.35; MALDI-TOF: m/z 1757.807 ([M]⁺).

Synthesis of Calix-4

Calix-3 (158 mg, 0.0899 mmol), 4-(diphenylamino)phenylboronic acid (156 mg, 0.3635 mmol), Pd(pph₃)₄ (31.2 mg, 0.0270 mmol), K₂CO₃ (278 mg, 2.16 mmol) aqueous solution were added to a flask under nitrogen atmosphere, and then dimethoxyethane (18 mL) was added. The reaction mixture was refluxed at 90 °C for overnight, and then was cooled and evaporated to dryness. The residue was dissolved in dichloromethane and the combined organic content was washed with water and saturated brines, and subsequently dried over anhydrous MgSO₄, filtered and evaporated to afford a crude product which was further purified by silica-gel column chromatography using petroleum ether and dichloromethane as the eluents (3:1, v/v) to yield 184.6 mg dark yellow solid. Yield: 85%. ¹H NMR (400 MHz, CDCl₃, δ): 7.36 (s, 4H), 7.34-7.31 (m, 14H), 7.28 (s, 4H), 7.22 (t, J = 8.0 Hz, 16H), 7.07 (d, J = 7.6

Hz, 16H), 7.01 (d, $J = 7.6$ Hz, 6H), 6.98 (s, 6H), 6.96 (s, 8H), 6.89 (s, 8H), 6.85 (d, $J = 3.6$ Hz, 4H), 6.75 (d, $J = 3.6$ Hz, 4H), 4.99 (s, 4H), 4.20 (d, $J = 13.2$ Hz, 4H), 2.97 (d, $J = 13.6$ Hz, 4H), 1.26 (s, 2H); ^{13}C -NMR (100 MHz, CDCl_3 , δ): 155.31, 147.53, 147.14, 143.15, 142.30, 137.44, 136.40, 135.71, 135.62, 129.94, 129.71, 129.41, 129.3, 128.64, 128.39, 128.30, 128.21, 126.35, 125.71, 124.65, 124.55, 124.51, 124.45, 124.23, 124.15, 123.78, 123.15, 122.94, 122.73, 76.81, 31.36; MALDI-TOF: m/z 2260.501 ($[\text{M} + \text{Na}]^+$).

Synthesis of HO-TPA

Calix-4 (500 mg, 0.207 mmol) was dissolved in dry toluene (25 mL), and then anhydrous AlCl_3 (331 mg, 2.48 mmol) was added and stirred at room temperature for 3 h. The residue was added with HCl (0.2 M) aqueous solution and then extracted with dichloromethane. The combined organic extracts were washed with water and brine, and subsequently dried over anhydrous MgSO_4 , filtered and evaporated to afford a crude product which was further purified by silica-gel column chromatography using petroleum ether and dichloromethane as the eluent (1:1, v/v) to yield 318 mg yellow green solid. Yield: 65%. ^1H NMR (400 MHz, CDCl_3 , δ): 10.23 (s, 4H), 7.43 (d, $J = 8.0$ Hz, 8H), 7.34 (s, 4H), 7.30 (s, 4H), 7.25 (s, 8H), 7.23 (s, 4H), 7.16 (d, $J = 7.6$ Hz, 8H), 7.10 (d, $J = 7.5$ Hz, 16H), 7.08-7.06 (m, 4H), 7.03 (d, $J = 7.4$ Hz, 16H), 7.01 (s, 4H), 6.98-6.84 (m, 4H), 4.32 (s, 4H), 3.63 (s, 4H); ^{13}C -NMR (100 MHz, CDCl_3 , δ): 148.65, 147.63, 147.52, 147.38, 142.93, 142.40, 136.44, 135.96, 130.11, 129.43, 129.36, 128.95, 128.67, 128.56, 128.17, 126.94, 126.46, 124.70, 124.63, 124.33, 123.72, 123.56, 123.23, 123.08, 122.98, 31.99; MALDI-TOF: m/z 2056.279 ($[\text{M} + \text{H}]^+$).

Determination of apparent quantum yield (AQY) in photocatalytic hydrogen production

The photocatalytic mixture was irradiated by an incident LED light source (Zolix, MLED4-1, M450L, $\lambda = 450$ nm, light intensity 100 mW cm^{-2} , irradiating area 0.8 cm^2) at 20°C . The number of incident photons was measured by a standard method using a

$K_3[Fe^{III}(C_2O_4)_3]$ actinometer and the photon flux was determined to be $1083 \mu\text{mol h}^{-1}$. The generated H_2 gas was analyzed by an Agilent 7820A gas chromatography with a thermal conductivity detector (TCD).

AQY (Φ) was calculated according to the following equation:

$$\phi = \frac{\text{number of transferred electrons}}{\text{number of incident photons}} \times 100\% = \frac{n(H_2) \times 2}{n(\text{photons})} \times 100\%$$

Determination of AQY in photoreduction of carbon dioxide

The apparent quantum yield (AQY) was measured using a band-pass filter ($\lambda_{\text{max}} = 450 \text{ nm}$, half width: 15 nm) and was estimated as follows:

$$\text{AQY}(\%) = (2 * N_{\text{CO-y}}) / N_{\text{ph}}$$

The $N_{\text{CO-y}}$ is the number of CO produced. The N_{ph} is the number of photon emitted from light source. The calculation of $N_{\text{CO-y}}$ is based on the fact that two photons are required to produce one molecule CO, according to the equations mentioned in the manuscript. The N_{ph} is calculated using the equation:

$$N_{\text{ph}} = [\text{Light intensity} \times \text{Illumination area} \times \text{Illumination time}]$$

/[Average single photon energy] where the light intensity is detected by irradiation meter, the illumination area is controlled to $1 * 0.7 \text{ cm}^2$, and the average single photon energy (E_{ph}) is figured out using the equation: $E_{\text{ph}} = hc/\lambda$. where h is the Planck constant, c indicates speed of light, and λ is the wavelength.

Determination of shedding amount of doped-dyes

10 mg catalyst Pt/Gel-TiO₂/HO-TPA (2.4 wt%) was dispersed and evacuated in 20 mL H₂O/TEOA (9:1 v/v) solution and then irradiated for 2 h, 4 h and 6 h under visible light ($\lambda > 420 \text{ nm}$), respectively. These samples were centrifugated and immersed in 5 mL THF. The obtained dye solutions were analyzed by UV-vis absorption spectra to give the dye shedding amounts according to the Labmert-Beer law.

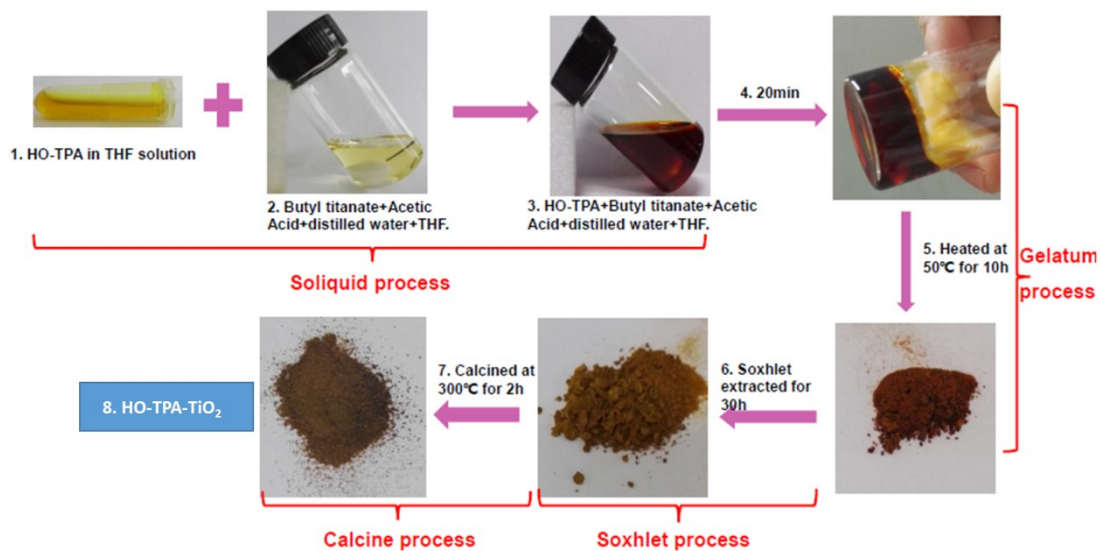


Fig. S2. Synthesis of HO-TPA-TiO₂ (5.0 wt%).

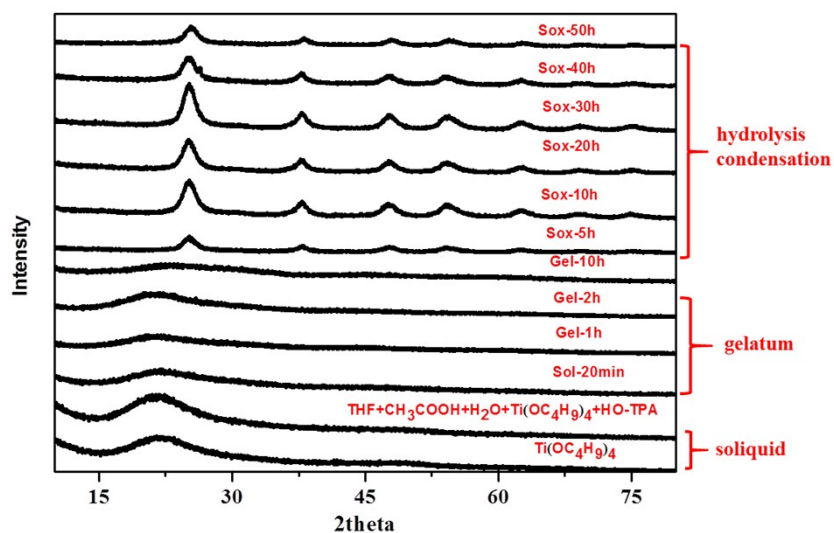


Fig. S3. XRD of the intermediaters at different reaction time before calcination in the formation process of HO-TPA-TiO₂ (5.0 wt%).

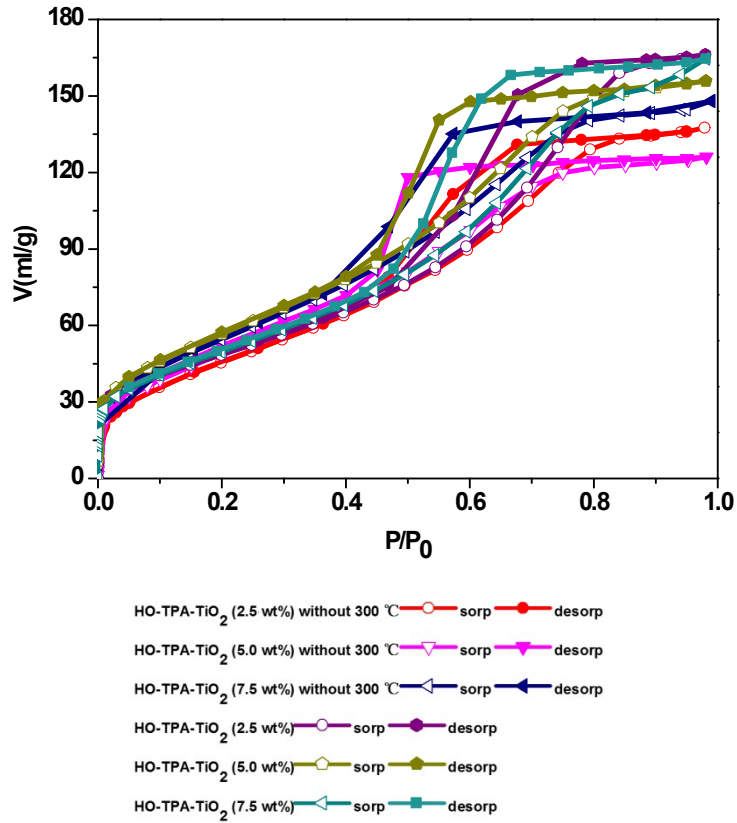


Fig. S4. N₂ adsorption-desorption isotherms of HO-TPA-TiO₂ (2.5/5.0/7.5 wt%) with and without 300 °C calcination measured under 77 K.

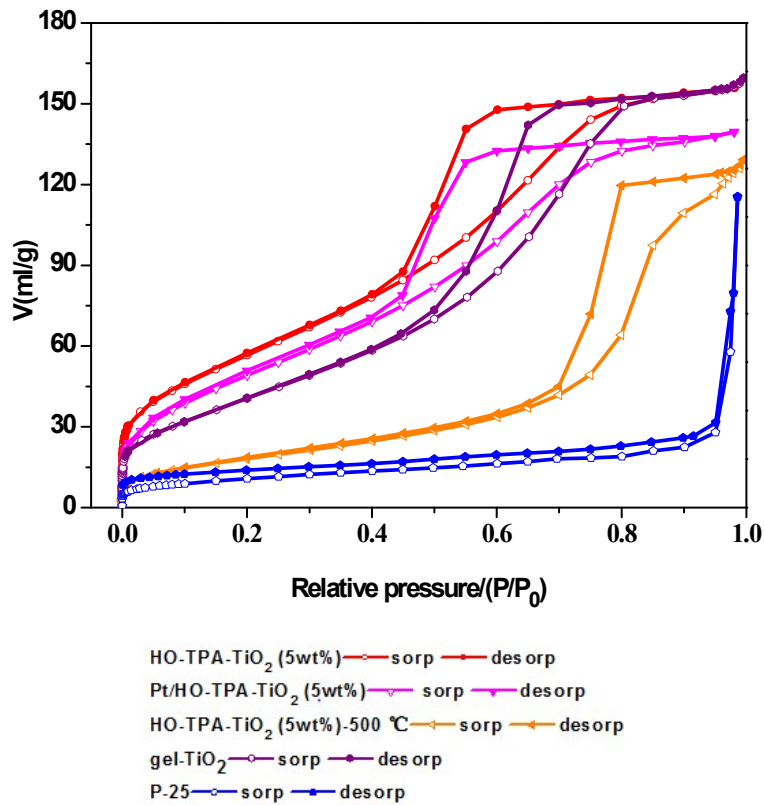
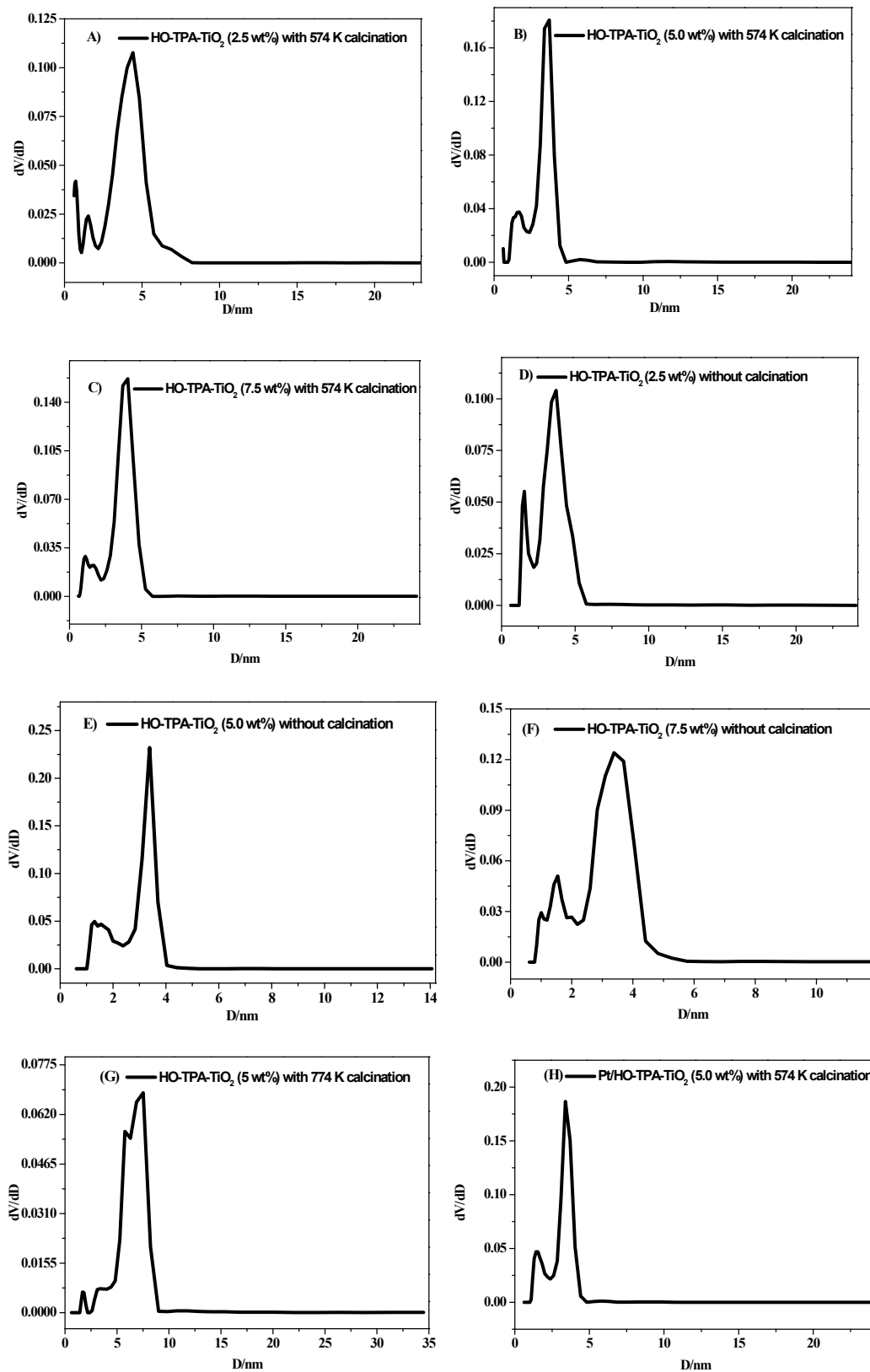


Fig. S5. N₂ adsorption-desorption isotherms of HO-TPA-TiO₂ (5.0 wt%) with 300 °C calcination, Pt/HO-TPA-TiO₂ (5.0 wt%) with 300 °C calcination, HO-TPA-TiO₂ (5.0 wt%) with 500 °C calcination, Gel-TiO₂ and P25-TiO₂ measured under 77 K.



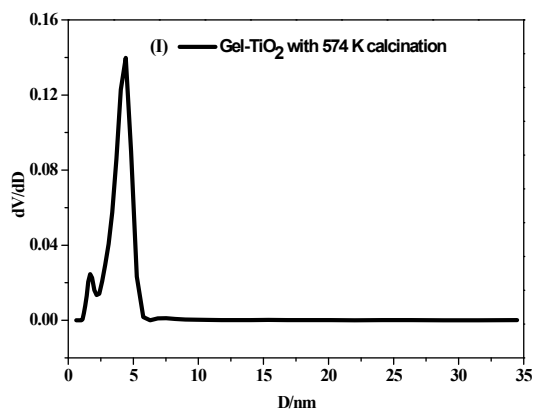


Fig. S6. The pore size distributions of HO-TPA-TiO₂ (5.0 wt%) system and Gel-TiO₂.

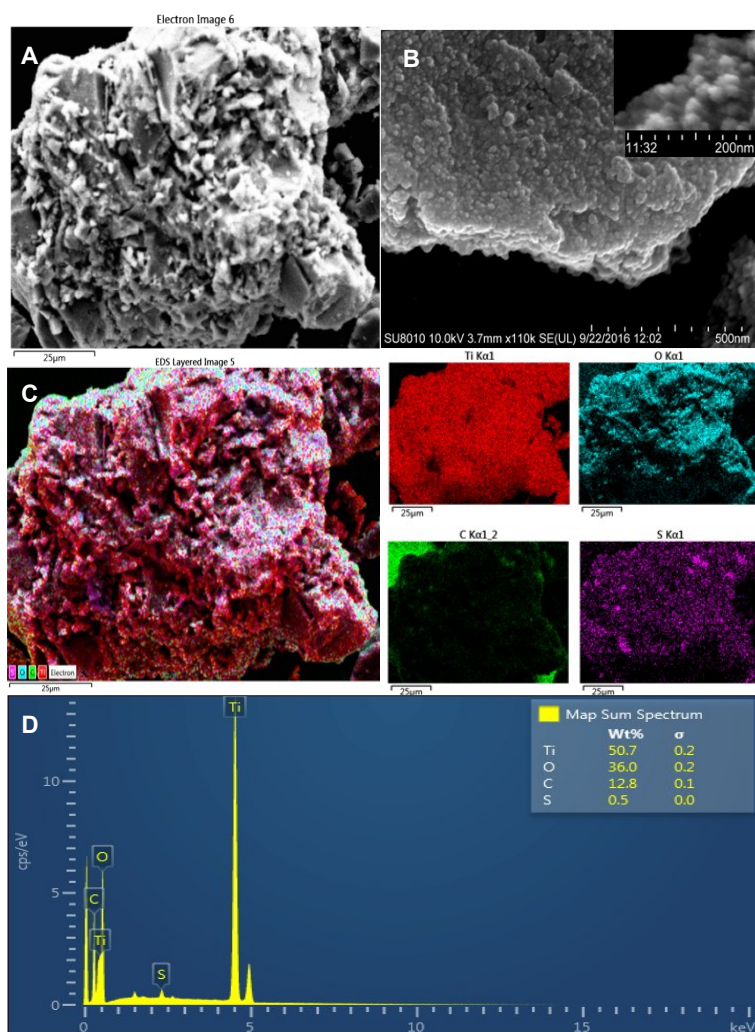


Fig. S7. (A) and (B) SEM, (C) and (D) the elemental mapping image, and (E) EDX of HO-TPA-TiO₂ (5.0 wt%).

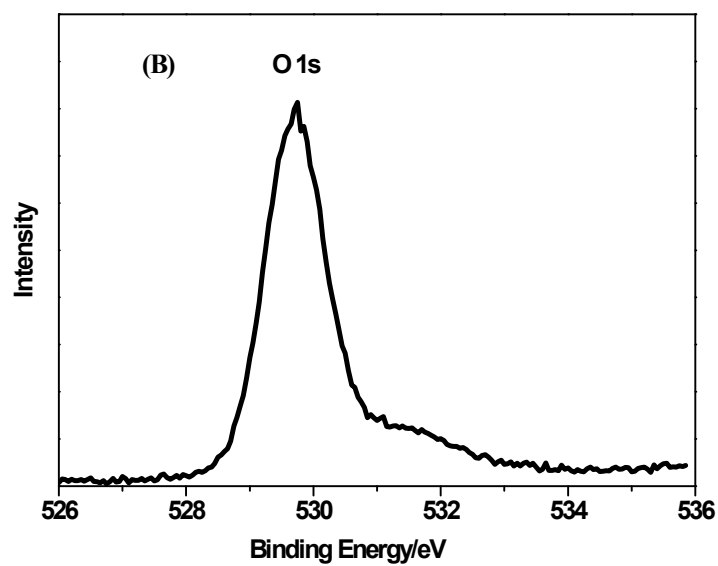
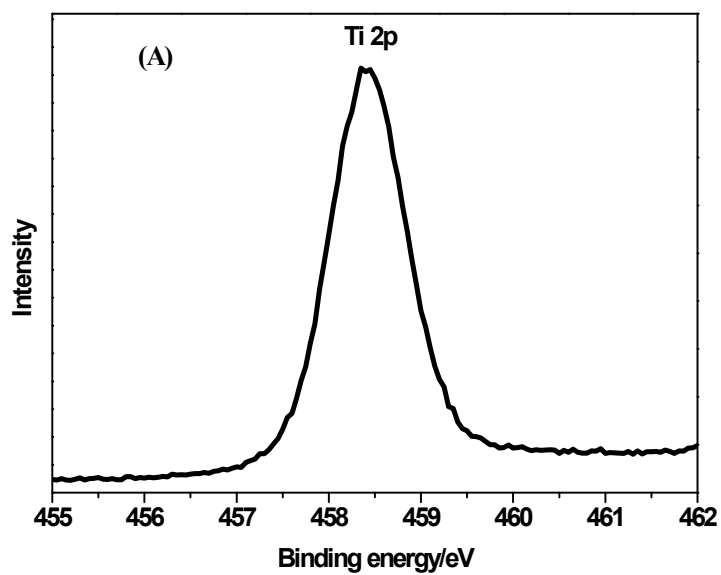


Fig. S8. X-ray photoelectron spectra for Ti and O of Gel-TiO₂. Atomic ratio of Ti : O = 25% : 52% \approx 1 : 2.

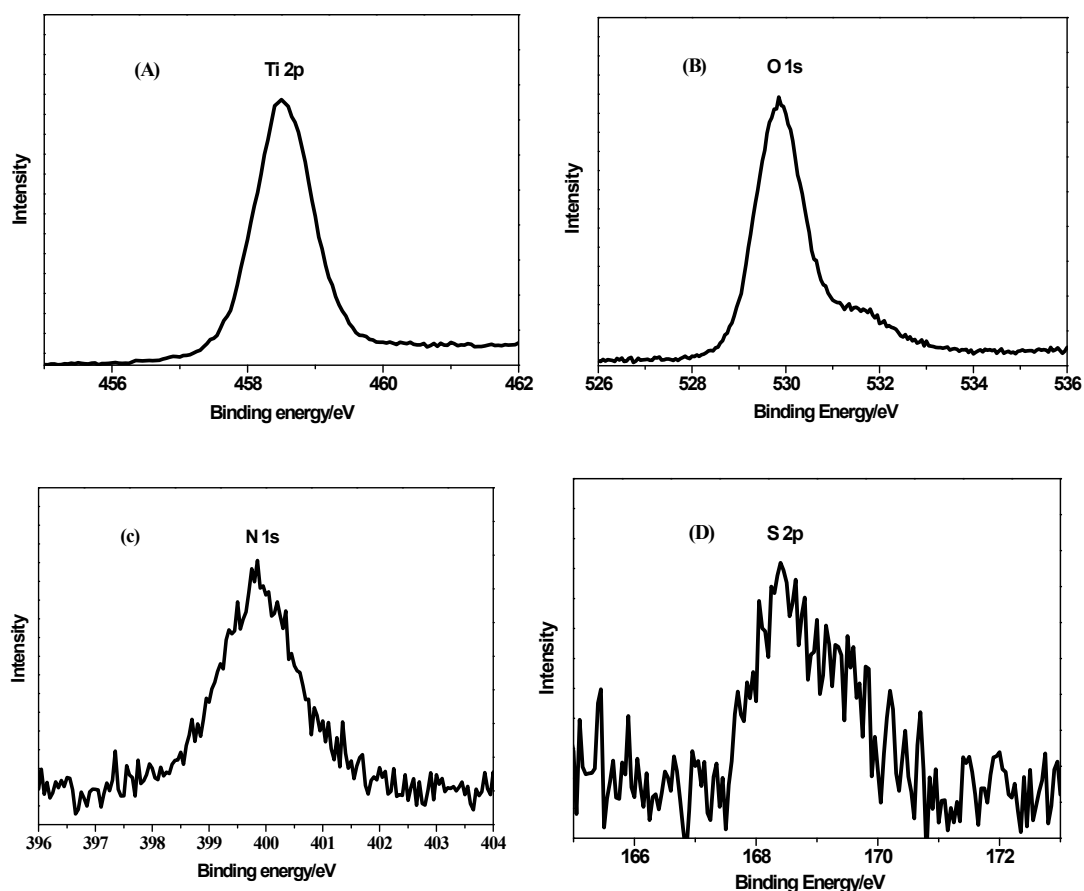


Fig. S9. X-ray photoelectron spectra for Ti, O, N and S of HO-TPA-TiO₂ (5.0 wt%). Atomic ratio of Ti : O : N : S = 24% : 53% : 1.91% : 0.67%.

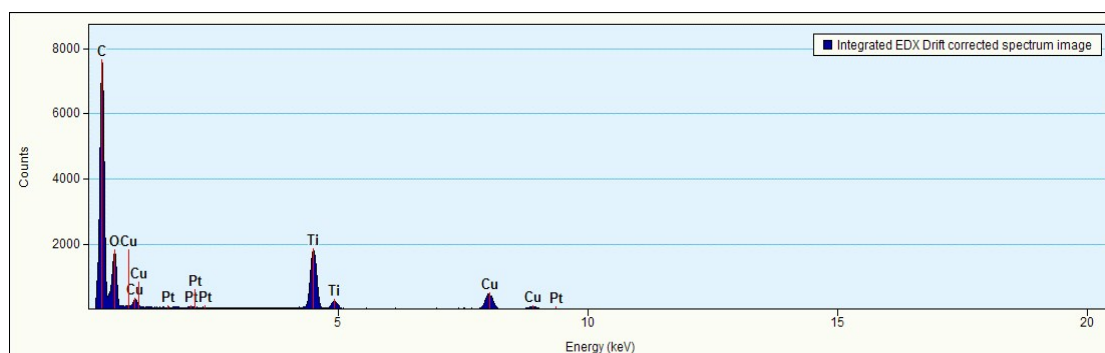


Fig. S10. EDX spectrum of Pt/HO-TPA-TiO₂ (5.0 wt%).

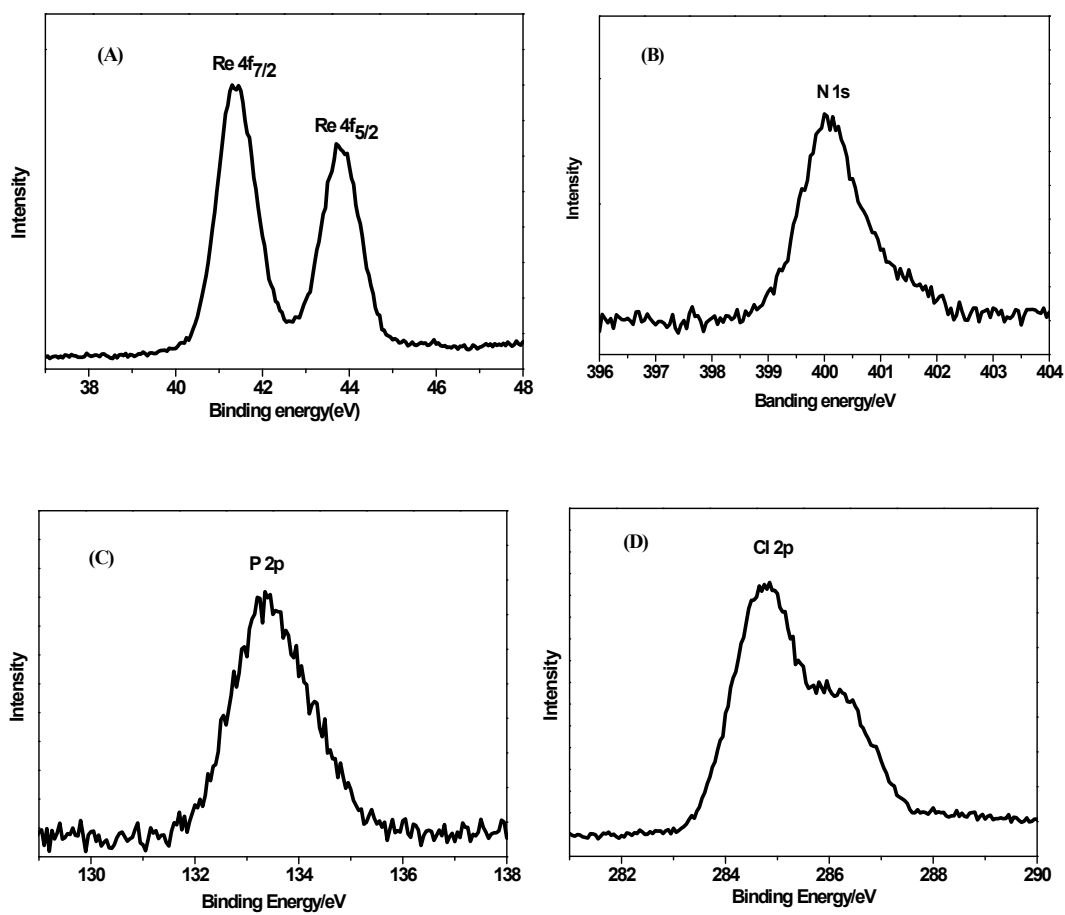


Fig. S11. XPS measurements for ReP. Atomic ratio of Re : N : P : Cl = 2.9% : 6.6% : 5.8% : 2.1% \approx 1 : 2 : 2 : 1.

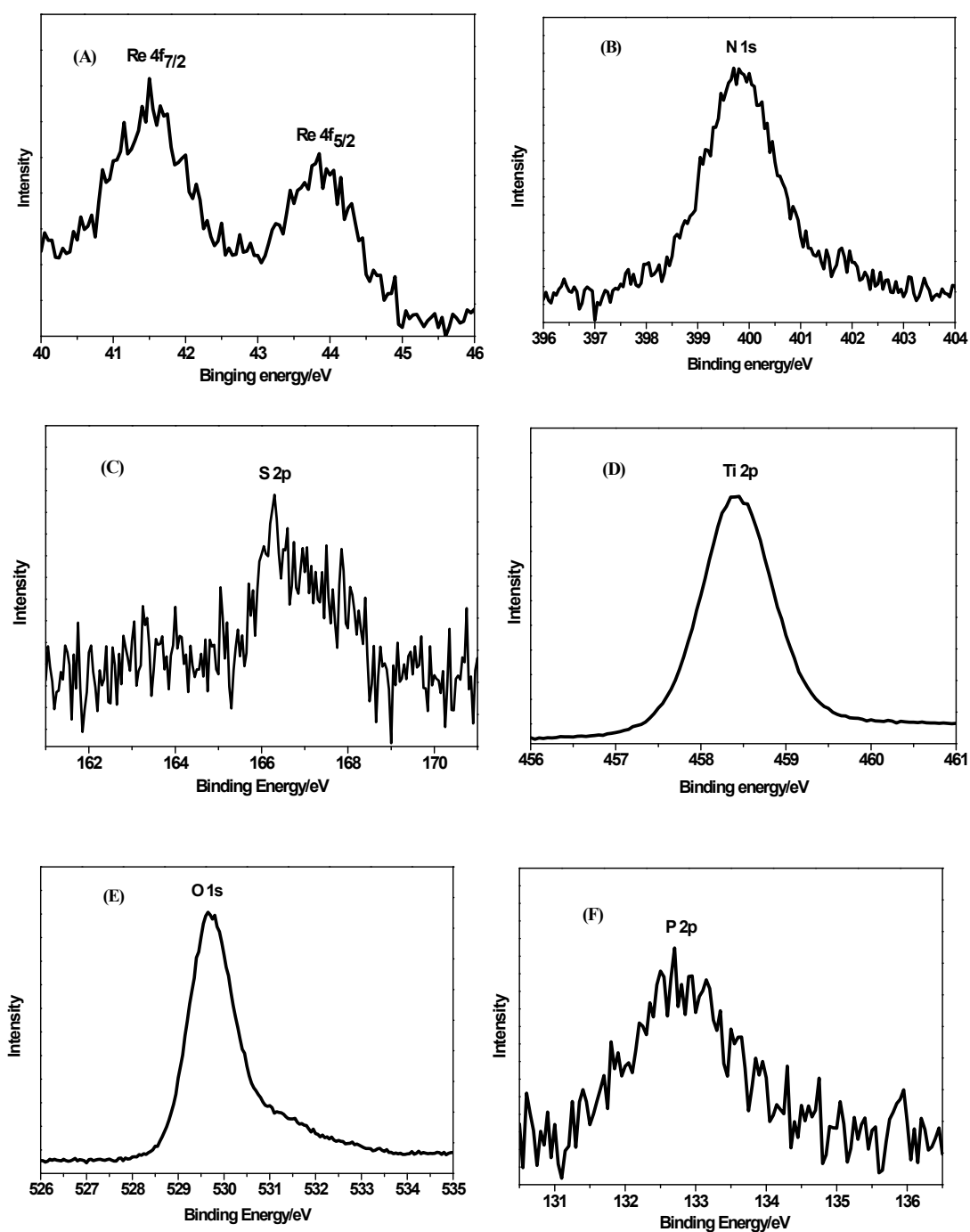


Fig. S12. XPS measurements for ReP/HO-TPA-TiO₂ (5.0 wt%) photocatalyst with 1.25 M TEOA as electron donor in 5 mL CO₂-saturated DMF after visible light irradiation for 24 h ($\lambda > 420$ nm). 10 mg catalysts were loaded with 0.041 μ mol ReP. Atomic ratio of Ti: O: Re: P: N: S = 23%: 51%: 0.29%: 0.56%: 2.8%: 0.43%.

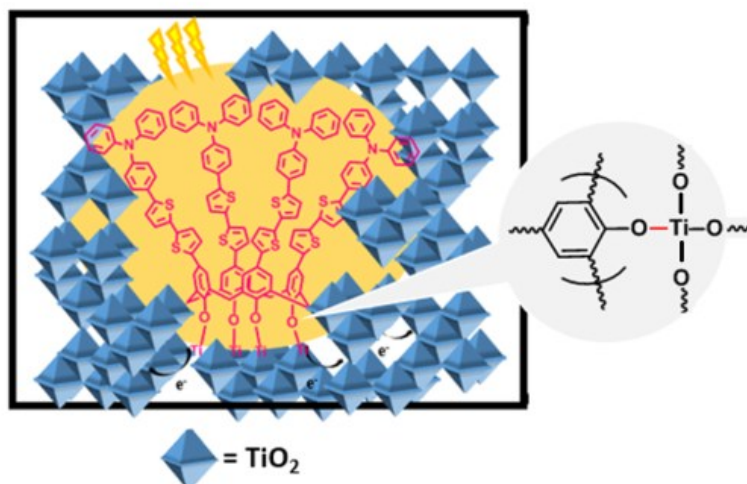


Fig. S13. The bonding mode between **HO-TPA** and TiO_2 .

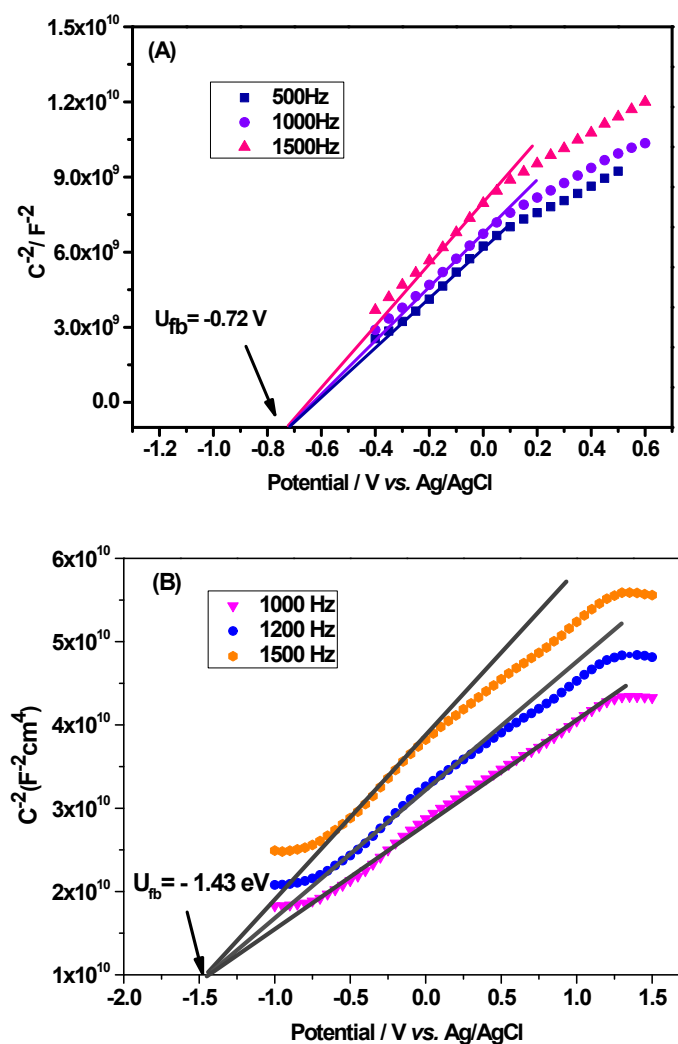


Fig. S14. Mott-Schottky plot of Gel- TiO_2 in (A) 0.2 M Na_2SO_4 aqueous solution and (B) DMF solution containing 0.1 M TBAP.

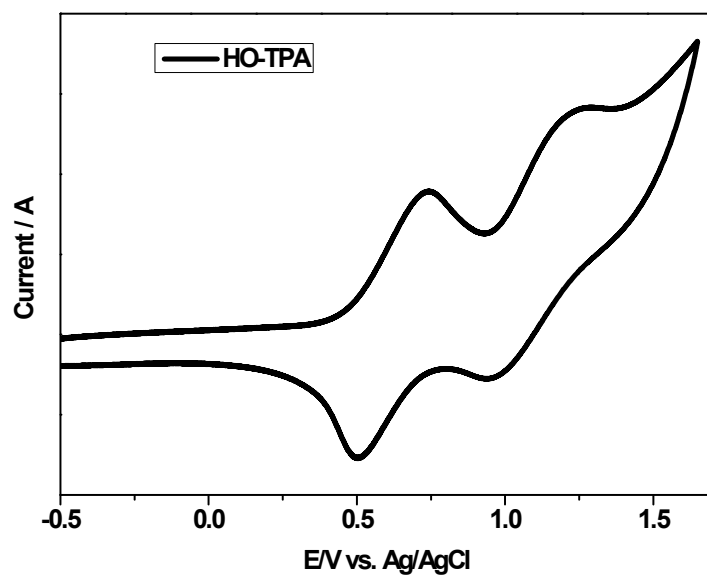


Fig. S15. Cyclic voltammogram of **HO-TPA** in 0.1 M TBAPF₆ of THF solutions measured with a scan rate of 100 mV s⁻¹.

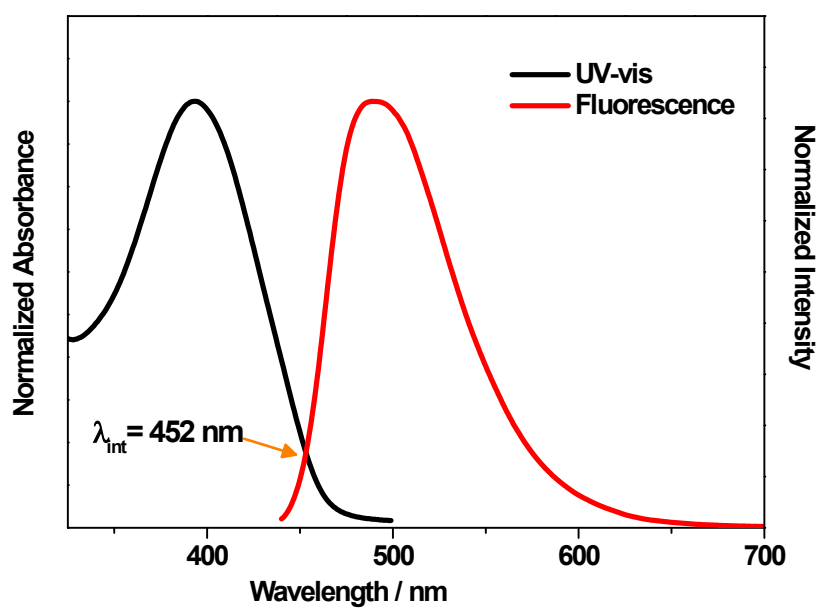


Fig. S16. UV-vis absorption spectra and photoluminescence spectra of **HO-TPA** in CH₂Cl₂ ($E_{0-0} = 1240/\lambda_{\text{int}}$).

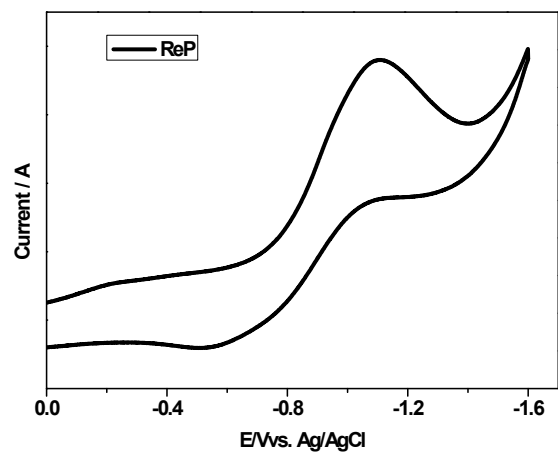


Fig. S17. Cyclic voltammogram of ReP in 0.1 M TBAPF₆ of THF solutions measured with a scan rate of 100 mV s⁻¹.

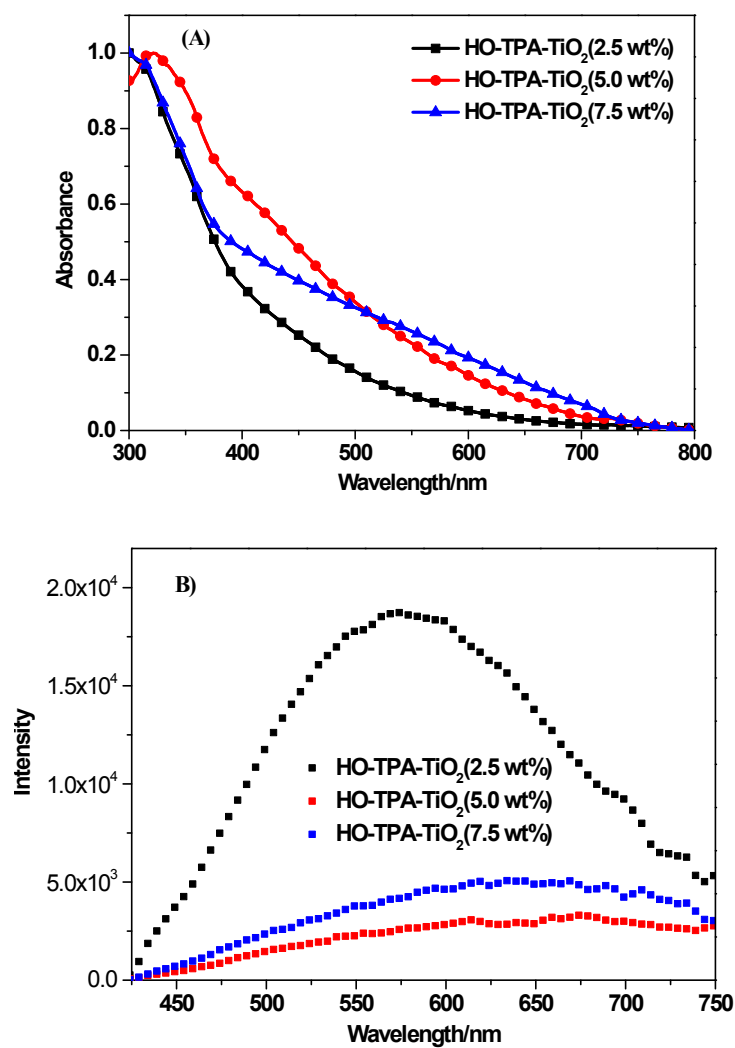


Fig. S18. (A) UV-vis diffraction and (B) steady-state solid photoluminescence spectra of HO-TPA-TiO₂ (2.5/5.0/7.5 wt%).

Experiment of doping-dye shedding

The corresponding characterization of dye doping shedding from the catalysts Pt/Gel-TiO₂/HO-TPA (2.4 wt%) and Pt/HO-TPA-TiO₂ (5.0 wt%) was evaluated by UV-vis absorption spectra. The shedding amounts of the dye for Pt/Gel-TiO₂/HO-TPA (2.4 wt%) were about 0.040 (0.82 wt%), 0.017 (0.35 wt%) and 0.016 (0.32 wt%) μmol for 2, 4 and 6 h under light illumination, respectively. The shedding dye amounts in reaction solutions decreased along with the increase of illumination time. One explanation could be that a portion of shedding dyes has degraded by photocatalyst under long-time illumination. As a control, the dye shedding from HO-TPA-TiO₂ (5 wt%) has not been detected under the same irradiation conditions. The color of the supernatant fluid in the photocatalytic system for Pt/Gel-TiO₂/HO-TPA (2.4 wt%) and Pt/HO-TPA-TiO₂ (5.0 wt%) was shown in Fig. S19. The color of the supernatant fluid based on Pt/Gel-TiO₂/HO-TPA (2.4 wt%) was yellow, while the reaction solution based on HO-TPA-TiO₂ (5 wt%) was colorless under the same illumination. The results indicated the hybrid materials had higher stability than common surface dye-sensitized system.

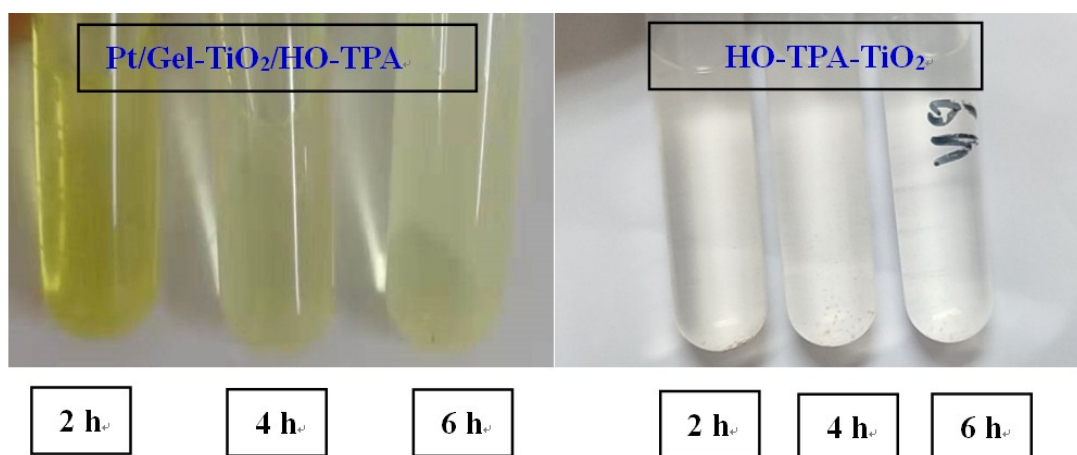


Fig. S19. The color of the dye doping shedding from Pt/Gel-TiO₂/HO-TPA (2.4 wt%) and HO-TPA-TiO₂ (5 wt%) after different time (2 h, 4 h and 6 h) illumination under visible light irradiation ($\lambda > 420 \text{ nm}$).

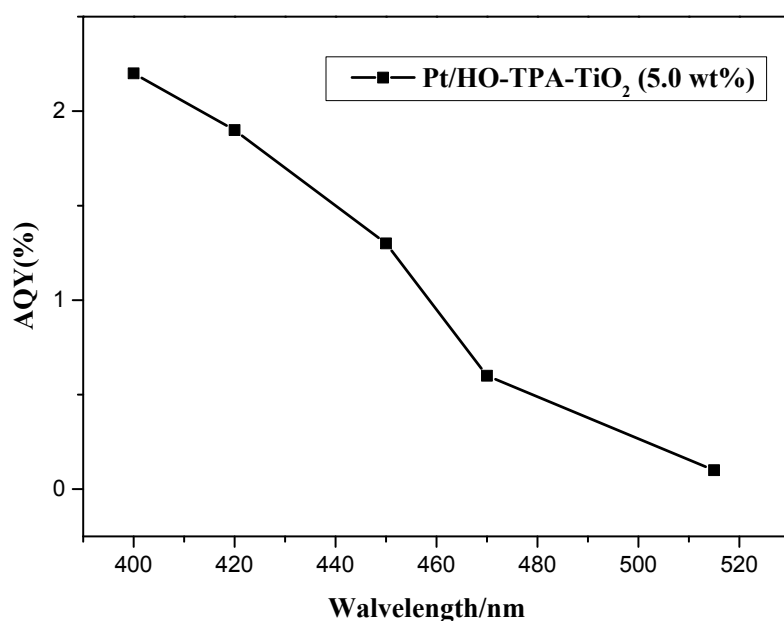


Fig. S20. Photocatalytic action spectrum for H₂ evolution after 1 h irradiation under 400, 420, 450, 470, and 515 nm LED light source.

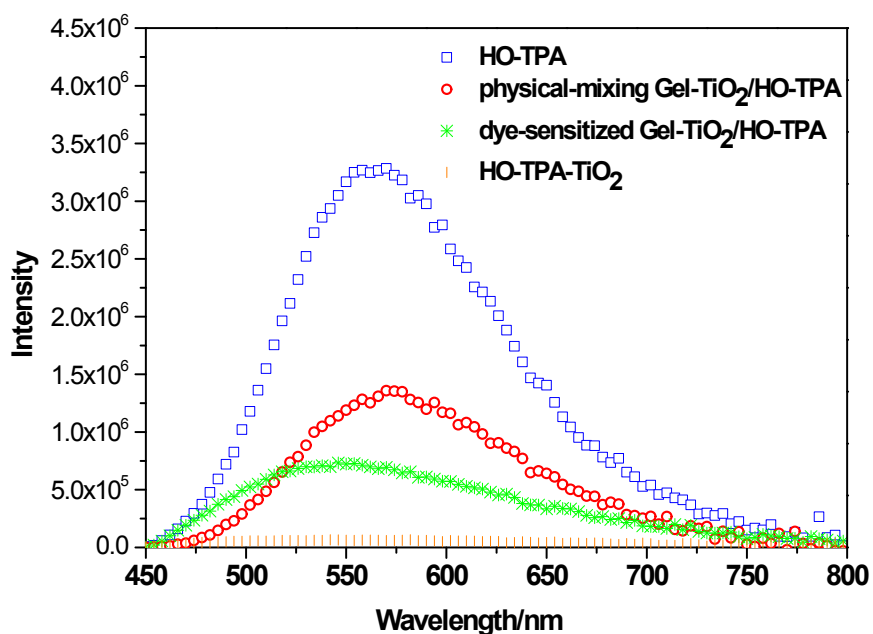


Fig. S21. Steady-state solid photoluminescence spectra of the HO-TPA, physical-mixing Gel-TiO₂/HO-TPA (5.0 wt%), surface dye-sensitized Gel-TiO₂/HO-TPA (5.0 wt%), and hybrid HO-TPA-TiO₂ (5.0 wt%).

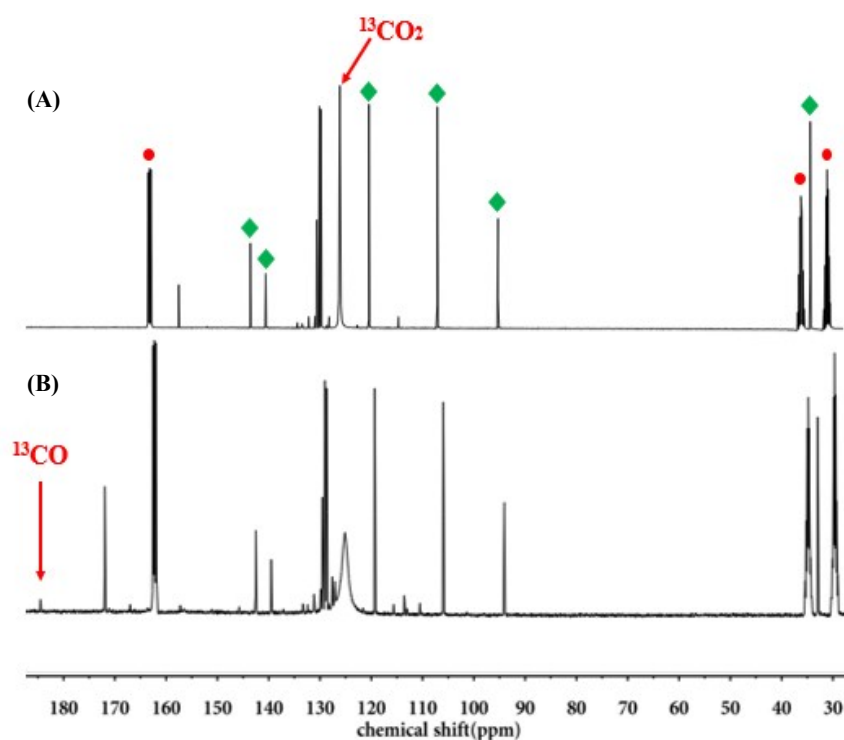
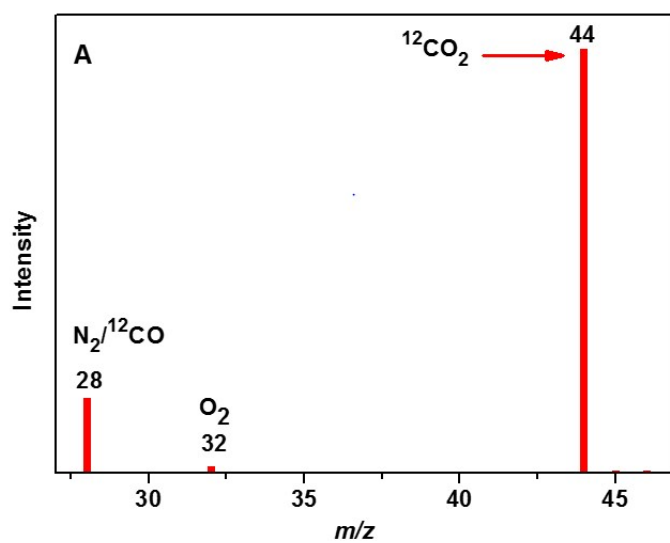


Fig. S22. ^{13}C NMR spectra of $^{13}\text{CO}_2$ and ^{13}CO before (A) and after (B) irradiation. CO_2 -saturated $\text{DMF-}d_7$ containing 10 mg of ReP/HO-TPA-TiO_2 (5.0 wt%) dispersion with 134 mg BIH under visible irradiation ($\lambda > 420$ nm) for 24 h. The symbols \blacklozenge and \bullet represent the peaks of DMF and BIH, respectively.



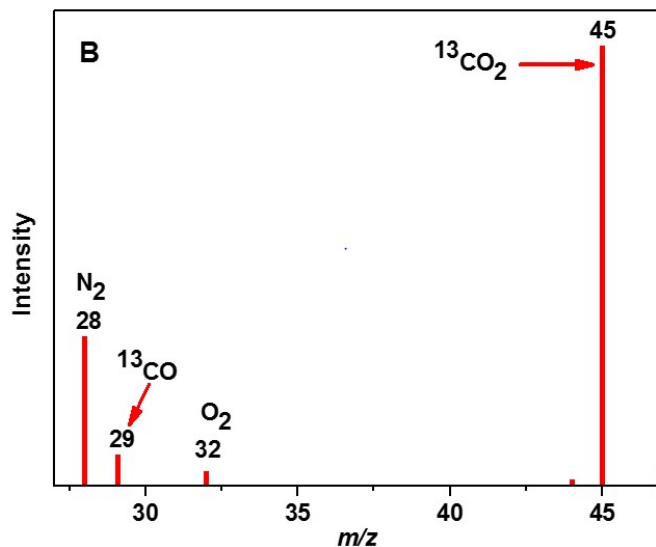


Fig. S23. GC-MS spectra of ReP/HO-TPA-TiO₂ (5.0 wt%) dispersion in (A) ¹²CO₂, and (B) ¹³CO₂-saturated DMF with BIH as the electron donor under visible light irradiation ($\lambda > 420$ nm) for 24 h.

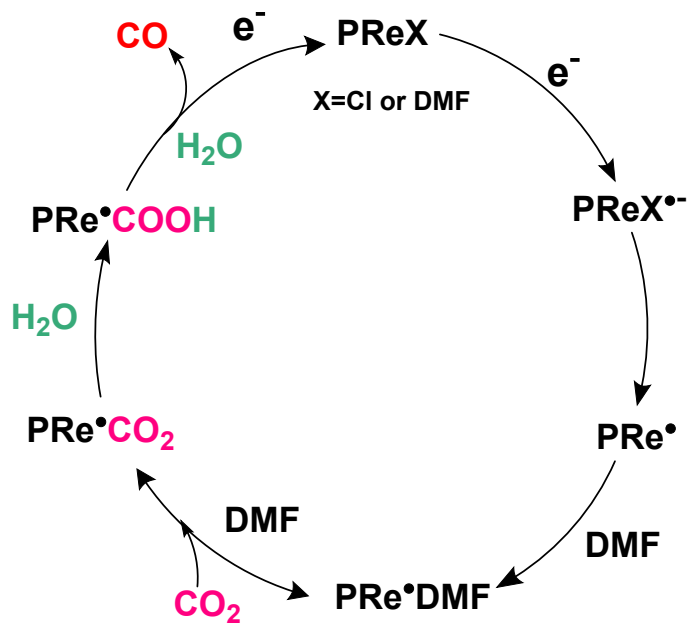


Fig. S24. Possible chemical processes for the two-electron reduction of CO₂ to CO catalyzed by a Re(I) complex (PReX).

Table S1. BET surface area, pore volume and pore width of HO-TPA-TiO₂ system derived from 77 K N₂ sorption isotherms.

Sample	Surface Area (m ³ /g)	Pore volume (ml/g)	Pore width (nm)	
			mesopore	micropore
P25-TiO ₂	55.40	0.162	29.40	
HO-TPA-TiO ₂ (5 wt%) with 500 °C calcination	68.42	0.176	7.52	1.83
HO-TPA-TiO ₂ (2.5 wt%) with 300 °C calcination	176.2	0.247	4.41	1.54
HO-TPA-TiO ₂ (2.5 wt%) without calcination	177.6	0.203	3.70	1.54
HO-TPA-TiO ₂ (5.0 wt%) with 300 °C calcination	184.7	0.218	3.70	1.68
HO-TPA-TiO ₂ (5.0 wt%) without calcination	188.4	0.214	3.39	1.54
Pt/HO-TPA-TiO ₂ (5.0 wt%) with 300 °C calcination	182.3	0.205	3.39	1.42
HO-TPA-TiO ₂ (7.5 wt%) with 300 °C calcination	188.9	0.244	4.04	1.10
HO-TPA-TiO ₂ (7.5 wt%) without calcination	210.4	0.214	3.39	1.54
Gel-TiO ₂ with 300 °C calcination	162.9	0.233	4.41	1.68

Table S2. Electrochemical properties of compounds used in this study (V vs. Ag/AgCl).

Compounds	Oxidation / V		Reduction / V		<i>E</i> ₀₋₀ / eV	<i>E</i> _{OX} [*] / V
	<i>E</i> _{ox}	<i>E</i> _{pc}	<i>E</i> _{Pa}	<i>E</i> _{1/2} ^{red}		
HO-TPA	1.24	-	-	-	2.74	-1.50
ReP	-	-1.11	-0.55	-0.83	-	-

Table S3. AQY results of Pt/HO-TPA-TiO₂ (5.0 wt%) after 1h irradiation under 450 nm LED light source.

Wavelength/nm	420	425	450	470	515
AQY	2.2%	1.9%	1.3%	0.6%	0.1%

Table S4. AQY results of some reported heterogeneous catalytic systems in photocatalytic H₂ production studies.

Catalyst	Sacrificial agent	Wavelength/nm	AQY/%	Reference
Pt/Calix-3-TiO ₂ (7.5%)	TEOA	450	2.9	Ref.1 (our work)
Dyad (dye)/Pt/TiO ₂	Ascorbic acid	420	1.3	Ref.2
TiO ₂ /Pt/Eosin-Y	TEA	520	10	Ref. 3
CdSe/MPA/TiO ₂	EDTA	450	0.6	Ref.4
TiO ₂ /Pt (alizarine) ₂	EDTA	500	0.5	Ref.5
NiS/Pt/TiO ₂ (black)	Methanol	420	5.4	Ref.6
TiO ₂ /Pt/ mecrocyanine dye	EDTA	517	1.8	Ref.7
TiO ₂ /Pt/ coumarin dye	NaI	440	2.5	Ref.8
1,1'- binaphthalene- 2,2'-diol/Pt/ TiO ₂	TEA	450	0.02	Ref.9
Pt/HO-TPA-TiO ₂ (5.0 wt%)	TEOA	420	1.9	This paper

Reference

- [1] J.-F. Huang, J.-M. Liu, L.-M. Xiao, Y.-H. Zhong, L. Liu., S. Qin, J. Guo, C.-Y. Su, *J. Mater. Chem. A*, 2019, **7**, 2993.
- [2] Y. Sun, Y. Sun, C. Dall'Agnesse, X.-F. Wang, G. Chen, O. Kitao, H. Tamiaki, K. Sakai, T. Ikeuchi, S. Sasaki, *ACS Appl. Energy Mater.*, 2018, **1**, 2813.
- [3] X. Liu, S. Min, Y. Xue, Y. Lei, Y. Chen, F. Wang, Z. Zhang, *Renew. Energ.*, 2019, **138**, 562.
- [4] R. Abe, K. Hara, K. Sayama, K. Domen, H. J. Arakawa, *J. Photochem. Photobiol. A*, 2000, **137**, 63.
- [5] V. S. Zakharenko, A. V. Bulatov, V. N. Parmon, *React. Kinet. Catal. Lett.*, 1988, **36**, 295.
- [6] P. Qiao, J. Wu, H. Li, Y. Xu, B. Sun, L. Ren, K. Pan, L. Wang, W. Zhou. *Nanotechnology*, 2019, **30**, 125703.
- [7] R. Abe, K. Sayama, H. J. Sugihara, *Sol. Energy Eng.*, 2005, **27**, 413.
- [8] R. Abe, K. Sayama, H. Arakawa, *Chem. Phys. Lett.*, 2002, **362**, 441.
- [9] S. Ikeda, C. Abe, T. Torimoto, B. Ohtani, *J. Photochem. Photobiol. A*, 2003, **160**, 61.

Table S5. The apparent quantum yields on photocatalytic CO production for ReP/HO-TPA-TiO₂ (5.0 wt%) at 420, 450 nm and 500 nm.

Wavelength /nm	N _{co-y}	N _{ph}	Light intensity/mW·cm ⁻²	Illumination time/s	AQY/%
420	9.544E+1 7	2.584E+2 0	17	7200	0.37
450	3.475E+1 7	2.769E+2 0	17	7200	0.13
500	3.077E+1 7	3.077E+2 0	17	7200	0.047